**Current Development in Oceanography**
Volume 5, Number 1, 2012, Pages 23-47
Published Online: November 2012
Available online at http://pphmj.com/journals/cdo.htm
Published by Pushpa Publishing House, Allahabad, INDIA

# CONCEPTUAL MODELS OF PACIFIC SARDINE DISTRIBUTION IN THE CALIFORNIA CURRENT SYSTEM

**Ricardo García-Morales[1], Bernardo Shirasago-Germán[1,*], Roberto Félix-Uraga[1] and Edgar Leonardo Pérez-Lezama[2]**

[1]Centro Interdisciplinario de Ciencias Marinas CICIMAR-IPN
Av. Instituto Politécnico Nacional s/n Col.
Playa Palo de Santa Rita Apdo
Postal 592, Codigo Postal 23096 La Paz, B.C.S., México
e-mail: bshirasago@ipn.mx

[2]Centro Regional de Investigación Pesquera, La Paz (Crip-La Paz)
Instituto Nacional de Pesca (INAPESCA)
Carretera a Pichilingue km1, S/N C.P.
23020 Col. Esterito, La Paz, Baja California Sur, México

## Abstract

Recent studies suggest that the ocean-atmosphere interactions can change drastically the ecosystem conditions as in the California Current System (CCS). The Pacific sardine population (*Sardinops sagax*) in the CCS is constituted by several stocks which present important variations in space and time. This study analyzed oceanographic surface variability in the California Current System by using satellite images and its influence in the distribution of sardine stocks. The monthly analysis of Sea Surface Temperature (SST) and



Keywords and phrases: Northeast Pacific, sardine catches, stocks, satellite images.

[*]Corresponding author

Communicated by Hyo Choi

Received August 1, 2012

Chlorophyll concentration "*a*" showed an important seasonal and interannual variability and the presence of mesoscale phenomena as cyclonic and anticyclonic gyres, upwellings and filaments that influences the sardine distribution and abundance. Three abundance peaks are observed from the analysis between sardine catch versus SST and Chl "*a*" data. For temperature, the first and highest peak was located below the 17°C, the second one between 17°C and 22°C, and the third one and the lowest above 22°C. This temperature range variation in space and time determines the latitudinal distribution of the stocks. For the catch and Chl "*a*" concentration analysis the first one and highest peak is delimited by the range from 0.6 to 1.8 mg/m$^3$, the second and the third one with many less catch between 1.8 mg/m$^3$ to 3.4 mg.m$^3$ and 3.4 to 6 mg/m$^3$. This Chl "*a*" concentration range variation in space and time determines the longitudinal distribution of the stocks, this means the distribution from the coastal to the oceanic zone.

## 1. Introduction

The California Current System (CCS) is a typical western boundary current characterized by an important seasonal variability and the presence of mesoscale phenomena such as coastal upwellings, cyclonic and anticyclonic gyres and filaments [7, 25]. This system consists of the California Current (CC) a dominant shallow (ca. 0-200m depth), wide (ca. 50-1000 km offshore) flow equator ward originated from the south of Canada and reaching the Baja California Peninsula (Mexico), with velocities about 25 cm/s [40, 45]. A portion of this current turns north to the south of Pt. Conception (~35° N) becoming the Southern California Countercurrent (SCC). This poleward current is matched at depth by the California Counter Current (CCC) a narrow (ca. 10-40 km) subsurface (ca. 200-400m depth) slope poleward countercurrent with velocities from 2 to 10 cm/s, carrying saltier and warmer water from Baja California (~31° N) to Vancouver Island (~50° N). Additionally, a surface poleward weak flow (ca. 5 cm/s) is originated in winter close to Pt. Conception named Davidson Current (DC) and travels north to at least Vancouver Island that in comparison with the CCC, the DC is generally broader (ca. 100km), stronger and it extends seaward of the slope [25, 35, 38]. On average, the CC is stronger in spring when it moves inshore, closer to the shelf-break. The CCC develops in the spring and persists through late fall. The DC dominates the flow over the shelf and beyond the shelf brake through winter.

The water masses present in the CCS are Subartic Water (SAW) with cold and relative low salinity values which are transported southward by the CC dominating in all the region [37], Surface Tropical Water (STW) and Surface Subtropical Water (SStW) located to the south and southwest of Baja California Peninsula [25, 31, 50], respectively. Other water masses present in the CCS are the Subsurface Equatorial Water (SsEW) carried poleward by the California Counter Current (CCC) [13] and the Intermediate Pacific Water (IPW) below 400m [46]. The dynamics of the CCS which affect the water masses distribution in space and time from weeks to even decades due to macroscale phenomena, generates different environmental conditions [44] that modulate the biological diversity and the chemical variability in the region [6, 15, 23].

On the other hand, the CCS region is affected by different winds fields. At high latitudes of the system (higher to 48° N) strong winds blow from the south in winter and weak ones from the north in summer. At mid-latitudes (35-48°N) winds have a strong seasonal cycle, being persistent from the north in summer and intermittent from the south in winter. At lower latitudes (25-35° N) winds are from the north on average but reach their strongest magnitude in the late spring [25]. Spring and summer northern winds drive offshore Ekman transport of surface waters, causing an upwelling of deeper cooler and more nutrient rich waters. The CCS also presents an important mesoscale activity characterized by gyres, meanders, filaments, jets and fronts being most of them an efficient offshore-inshore interchange mechanism [15, 18, 27, 31, 42, 43]. This mechanism accumulates and maintains many species of plankton in the open ocean [4], and influences the CCS ecosystem especially over the population dynamics of the Pacific sardine (*Sardinops sagax*).

Several studies on marine communities have shown that the species distribution depends on the environmental variability and therefore its parameter has been used as indicators of a particular habitat [16]. The sardine distributes in highly productive current systems as the case of the CCS [24, 36]. The fishery richness in the region is a consequence of the high levels of productivity produced by the coastal upwellings generating high levels of nutrients in the euphotic zone [2].

The Pacific sardine distribution in the CCS varies depending on its abundance. When the population is very high, its distribution is from the southeast of Alaska to the southern part of the Baja California Peninsula including the Gulf of California, dominating the neritic zone of the ocean [28, 36]. The Pacific sardine population is constituted by several stocks and this fact is sustained in part by the presence of several spawn areas separated geographically [36], tagging information [9], vertebral counts [10, 47], blood groups [47, 48] morphometric data [12, 22, 48], genetics [24, 26, 29], and catches-Sea Surface Temperature (SST) analysis [20, 21]. The studies about geographical distribution of the sardine in the CCS sustain the existence of three stocks. However many uncertainties exists about the limits of these stocks, mainly for the most northern stock which could be fractioned in two groups, one spawning in Oregon-Washington offshore and another in front of Southern California coast [17, 44].

The analysis of environmental variability is important to describe changes in the population abundance of Pacific sardine. The massive growth of this population is associated to warm periods with moderate coastal upwellings [29].

The biological production as a result of coastal upwellings differs of the one originated by the curl-driven upwellings in the open ocean. The coastal upwellings present higher vertical speeds resulting in larger phytoplankters, while the curl-driven upwellings with low vertical speeds favoring smaller phytoplankters [19, 32], however this open ocean upwellings also contributes with nutrients to the pelagic ecosystem [49, 13, 39].

Rykaczewski and Checkley [41] compared coastal upwellings and curl-driven upwellings occurring offshore with the sardine population production. Results indicated that the curl-driven ones had a significant correlation with the sardine production and not with the coastal ones in the same period. On the other hand, Checkley, Jr. et al. [8] indicate the sardine spawns occur mainly offshore in the frontal zone of the coastal upwelling.

Zwolinski et al. [52] carried out a presence-absence analysis of sardine eggs related to sardine catches and SST and Chlorophyll "*a*" concentrations (Chl "*a*"). They developed a widespread preservative model (GAM) to predict space-time distribution patterns and the habitat of the northern sardine in the CCS. The results showed that the sardine eggs are distributed at SST from 11.5 to 15.5°C and Chl "*a*" from 0.18 to 3.2 mg/m3. The model results also indicated that the maximum probability of sardine presence is approximately at SST of 13.2 °C and Chl "*a*" of 0.5 $mg/m^3$.

The characterization of the different ecosystems along of the CC is necessary for the understanding of the distribution of the Pacific sardine stocks. Therefore, this study is focused in the analysis of Pacific sardine catches and their relation with the SST and Chl "*a*", as well as the presence of mesoscale structures in six areas located in the northwestern Pacific. The study was developed with the hypothesis that the Pacific sardine habitat in the oriental border of the California Current System is determined by the seasonal and interannual variability of the environment evaluated through some parameters such as SST, Chl "*a*", and the presence of mesoscale structures.

## 2. Materials and Methods

### 2.1. Study site

The study site is located in the California Current System from the 22°N to 46ºN and from 109°W to 132°W approximately. The site was divided in six fishing areas of Pacific sardine: Magdalena Bay (MB), Cedros Island (CI), Ensenada (EN), San Pedro (SP), Monterey (MY), Oregon and Washington (O-W). Four most representative quadrants from each area were selected taking into account the maximum variation of SST and Chlorophyll "*a*". The values of these four quadrants were averaged to obtain a characteristic value of each one of the six mentioned areas (Figure 1).

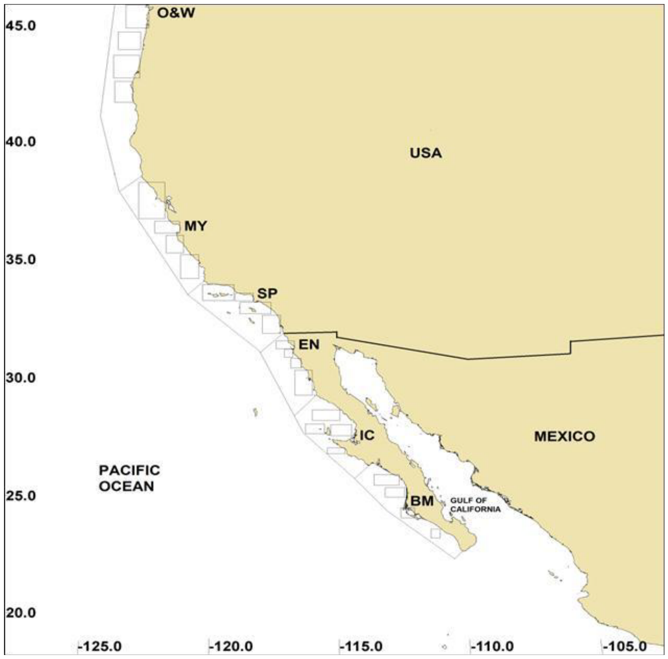


**Figure 1.** Fishing areas and quadrant selection. Magdalena Bay (MB), Cedros Island (CI), Ensenada (EN), San Pedro (SP), Monterey (MY), Oregon and Washington (O&W).

### 2.2. Database

300 monthly averaged SST images were used in this work derived from NOAA-AVHRR sensor (National Oceanic and Atmospheric Administration - Advance Very High Resolution Radiometer) for the years 1981-2000, and MODIS (Moderate Resolution Imaging Spectroradiometer) - Aqua/Terra composite images for 2001-2005. 168 monthly averaged chlorophyll "*a*" concentration images were used derived from CZCS (Coastal Zone Color Scanner) for the years 1981-1986, OCTS and SeaWIFS (Be-viewing Wide Field-of-view Sensor) for 1997 to 1999 and MODIS-Aqua/Terra-MERIS (Medium Resolution Imaging Spectrometer) composite images for 2000-2005. Satellite data were derived from different sensors in order to increase coverage and diminish missing data. Most of the images are in high resolution (1.1 km in the Nadir) and HDF (Hierarchical Data Format). These data were supplied by Scripps Institution of Oceanography.

The satellite images were cut for selecting the study areas, fishery zones, and averaged quadrants for further analysis with catches. The seasonal mesoscale gyre maps were constructed by means of standard visual procedures detecting structures with SST and Chl “*a*” gradients [33, 34], but taking into account that the chlorophyll concentrations were only available for the periods 1981-1986 and 1997-2005. These satellite image works were done by using the WIM software (Windows Image Manager).

Monthly data of sardine catches (1981-2005) in Magdalena Bay (MB), Cedros Island (CI) and Ensenada (EN) were obtained from the Population Dynamics Laboratory of the Interdisciplinary Center of Marine Sciences (CICIMAR-IPN), based on the records registered from sardine processing factories that operate in this fishing areas. The catches data of San Pedro (SP), Monterey (MY) and Oregon-Washington (O-W) were provided from the Southwest Fisheries Science Center (SWFSC) at La Jolla, California. All data collected were used as indicators of availability and abundance of the sardine stocks.

### 2.3. Conceptual models

Three distribution conceptual models were elaborated with seasonal averages of catches, and SST, Chl “*a*” satellite images, as well as the presence of mesoscale gyres to describe the space-time distribution of the sardine stocks in the CCS based on the conceptual model proposed by Félix-Uraga et al. [20, 21]. The Felix-Uraga model was modified for this study to include SST and Chl “*a*” satellite data and mesoscale gyres, as well as catch data of 2003-2005 and fishing areas of MY – O-W. The conceptual models were overlaid over 2003 seasonal images of SST and also compared with seasonal Chl “*a*” and mesoscale gyres maps because this year represents an oceanographic typical year and it showed the seasonal phenomena characteristic of the region. The three models were used to describe some environmental characteristics that describe the distribution of the temperate and cold stocks. The warm stock was excluded from the conceptual models because of its very limited presence.

## 3. Results

### 3.1. Sardine catches vs. SST and Chl "*a*" analysis

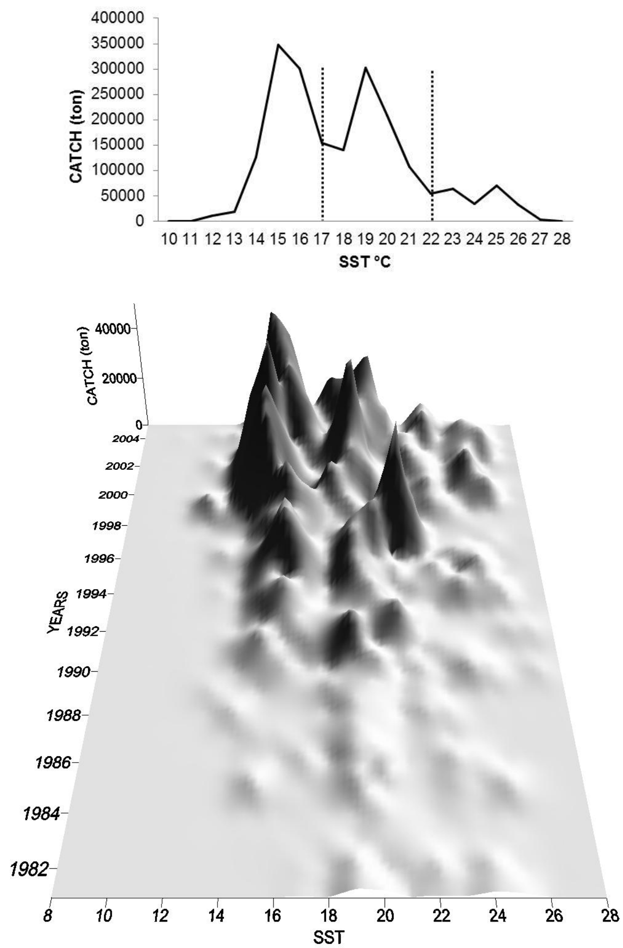


**Figure 2.** Total catches of Pacific sardine vs. SST in the CCS fishing zones. (a) Total catches for 1981-2005 period, (b) Annual distribution.

Three stocks in the CCS are observed in the annual distributions of the total catches (Figures 2a, 2b). The first one adapted to higher temperatures than 22°C (warm stock), the second one between 17°C and 22°C (temperate stock) and the third one to lower temperatures than 17°C (cold stock).

In the case of the total catches and Chl "*a*" showed a catch maximum at 0.6 mg/m$^3$ surface concentrations, with a gradual catch decrease toward higher concentrations (Figure 3a). Longitudinal distribution of sardines shows higher catches offshore and lesser ones in the coastal zone (Figure 3b).

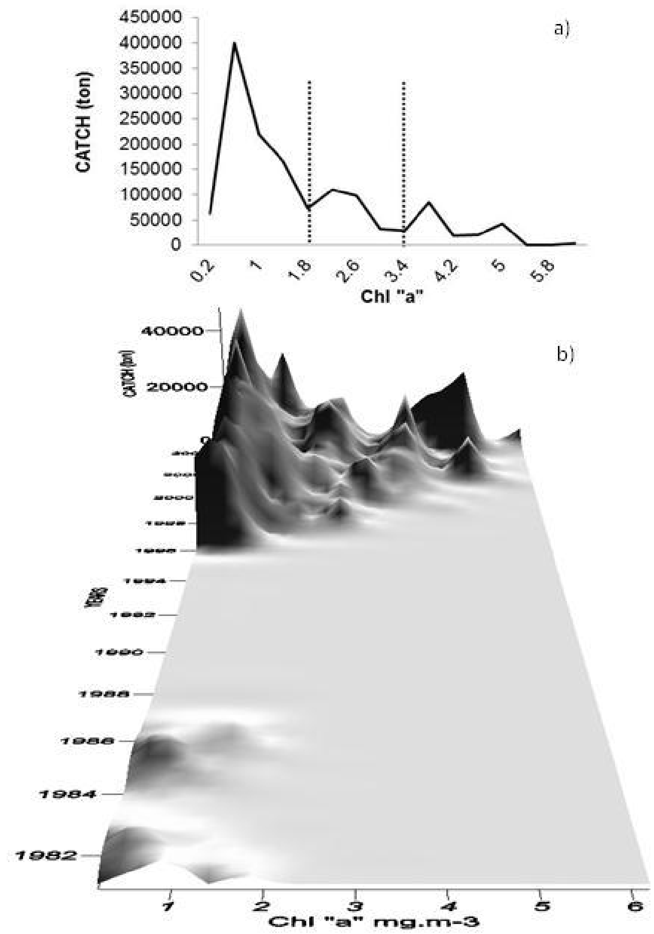


**Figure 3.** Total catches of Pacific sardine vs. Chl "*a*" in the CCS fishing zones. (a) Total catches for periods 1981-1986 and 2000-2005, (b) Annual distribution.

**3.2. Monthly variability analysis per fishing zones of SST, Chl "*a*" and catches for the temperate and cold stocks**

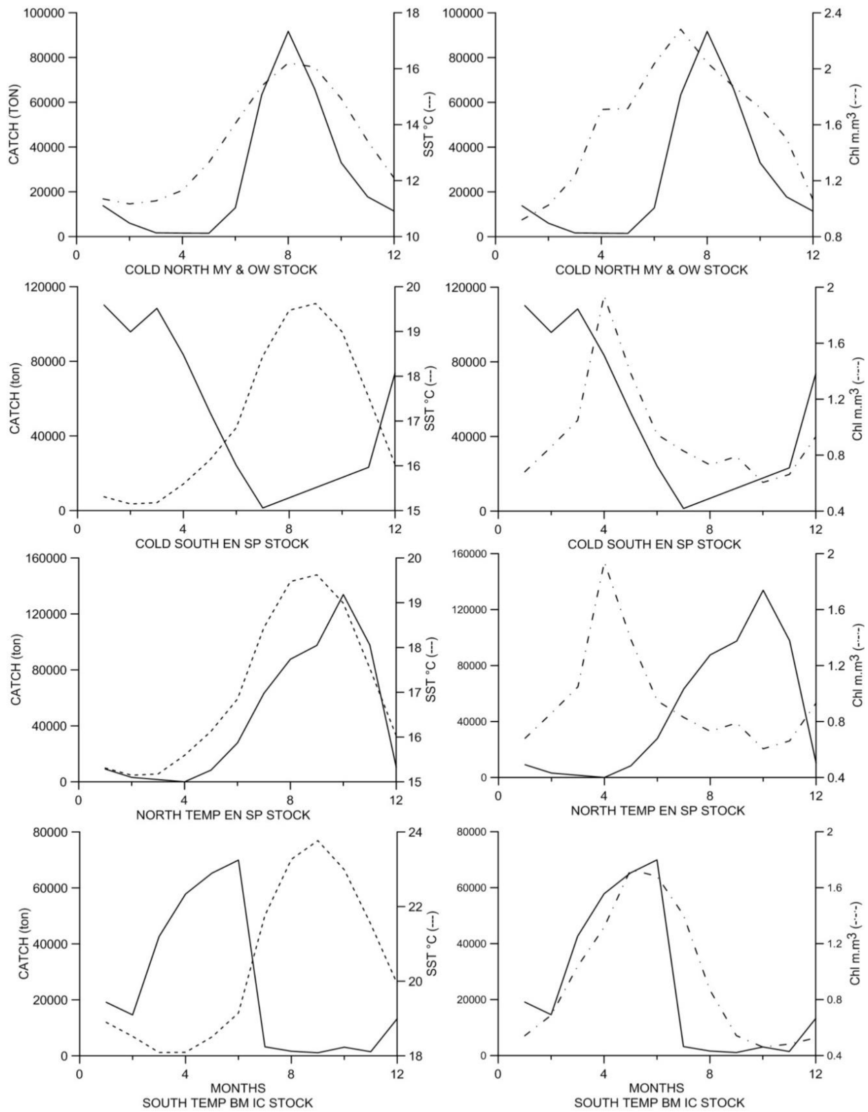


**Figure 4.** Monthly variation of catches, SST and Chl "*a*" for the temperate and cold stock (north and south distribution zones). The continuous lines indicate the monthly catches, the dotted line the SST and the dotted-dashed line the Chl "*a*".

After excluding the warm stock our analysis showed that when the temperate stock is located to the southern side of its distribution zone (MB and CI) the higher catches occurred in the first half of the year. When the temperate stock is to the northern side of its distribution zone (IN and SP) the higher catches occur in the second part of the year. In both cases the temperate stock is restricted to SST between 17°C and 22°C and Chl "*a*" between 0.4 and 1.8 mg/m$^3$. It is noticeable the synchronization between both higher values of catches and chlorophyll concentration in the first half of the year while in the second part of the year this phenomenon is not observed (Figure 4).

A similar situation was observed with the cold stock, when it is located to the southern side of its distribution zone (EN and SP) the higher catches occur in the first half of the year. When its distribution is present in the northern side (MY and O-W) the higher catches occur in the second part of the year. In both cases the cold stock is restricted to SST lower than 17 °C and Chl "*a*" between 0.4 and 1.8 mg/m$^3$. In this case the higher catches are associated to higher values ranges of Chl "*a*" (Figure 4).

### 3.3. Conceptual models of the Pacific sardine distribution related to SST, Chl "*a*" and mesoscale phenomenology

The conceptual models of catches-SST images delimited the latitudinal distribution pattern for both stocks, meanwhile the conceptual models of catches-Chl "*a*" delimited the longitudinal distribution pattern for the stocks.

**3.3.1. Winter.** According to the catches-SST model for this season (Figure 5a) both stocks are located to the north of their distribution zone. The cold stock is distributed mainly along the coast from MY to O-W in areas with SST values below the 17°C. The temperate stock is located from BM to the south of EN and mainly in areas with SST values between the 17°C and 22°C. The higher catches of this season were in MY (cold stock) and in MB (temperate stock).

The catches-Chl "*a*" model presented longitudinal variations of Chl "*a*" being higher in the coast and lower in the open ocean. The higher catches were obtained in the range from 0.6 to 1.8 $mg/m^3$. This range is restricted to the coastal zone with the exception of a broad area to the north of MY where the 0.6 $mg/m^3$ values are found offshore (Figure 5b).

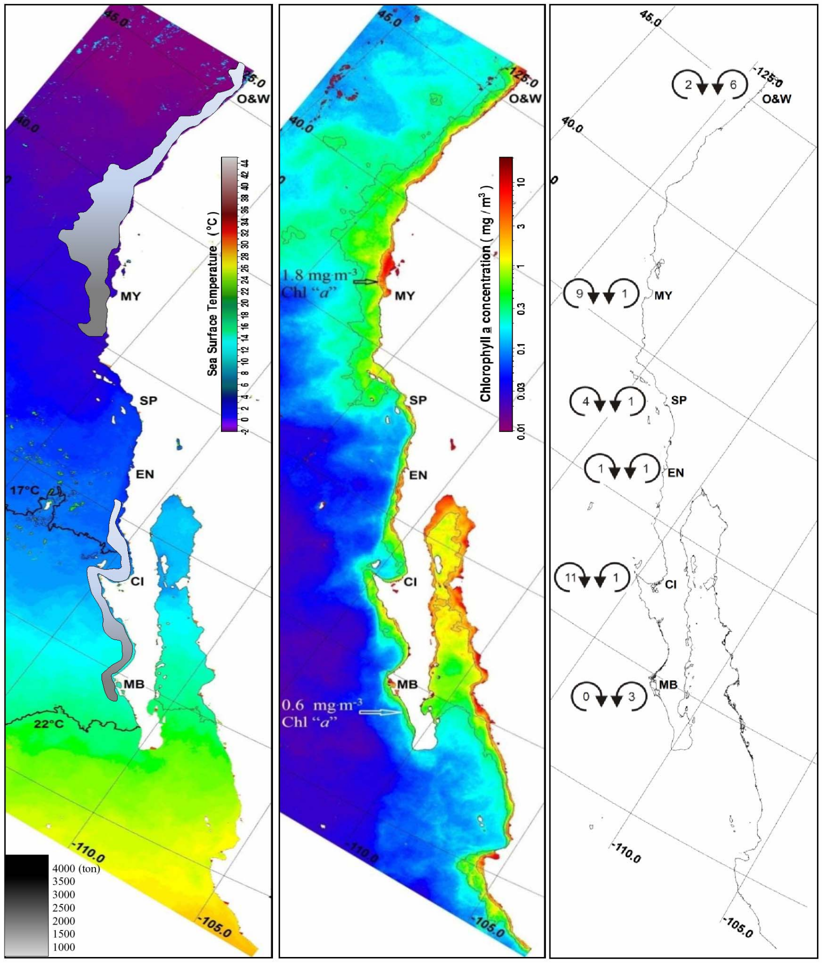


**Figure 5.** Conceptual models of sardine catch distribution for SST and Chl "*a*" (overlaid on winter 2003 images), and mesoscale phenomena for winter. (a) SST seasonal average image overlaid with the stock distribution patterns, and 17°C and 22°C isotherms. (b) Chl "*a*" image with 0.6 and 1.8 $mg/m^3$ isolines. (c) Frequency of mesoscale cyclonic and anticyclonic gyres of each fishing area.

The number of cyclonic and anticyclonic gyres generated during winter of all analyzed years in each fishing area is shown in Figure 5c. The anticyclonic gyres were the most frequent mesoscale phenomena present in the study site with the exception of O-W and MB, where the cyclonic gyres dominated. The mayor presence of these phenomena was observed in the CI area (12 gyres) and the minor in the MB area (3 gyres). Moderated upwellings and filaments were also observed by means of the Chl "*a*" images mainly between SP and O-W.

**3.3.2. Spring.** The models shown that the two stocks reach their southernmost distribution in this season (Figure 6a). The cold stock is distributed mainly along the coast from MY to the south of EN and also in areas with SST values below the 17°C. The temperate stock is located from CI to the southern zone of MB and also in areas with SST values between 17°C and 22°C. The higher catches of this season were in EN (cold stock) and MB (temperate stock).

The catches-Chl "*a*" model in this season presented the same longitudinal pattern than in winter but with higher Chl "*a*" near the coast and also registering the higher catches offshore between 0.6 to 1.8 mg/m$^3$ (Figure 6b).

The generation of cyclonic and anticyclonic gyres varies in spring in comparison to winter increasing from CI to EN and decreasing in O-W and MY dominating again the anticyclonic gyres (Figure 6c). The mayor presence of these phenomena was observed in CI area (24 gyres) and the minor one in the MB area (3 gyres). The intensity of upwellings and filament dimensions increased in this season mainly in the north part of the study area.

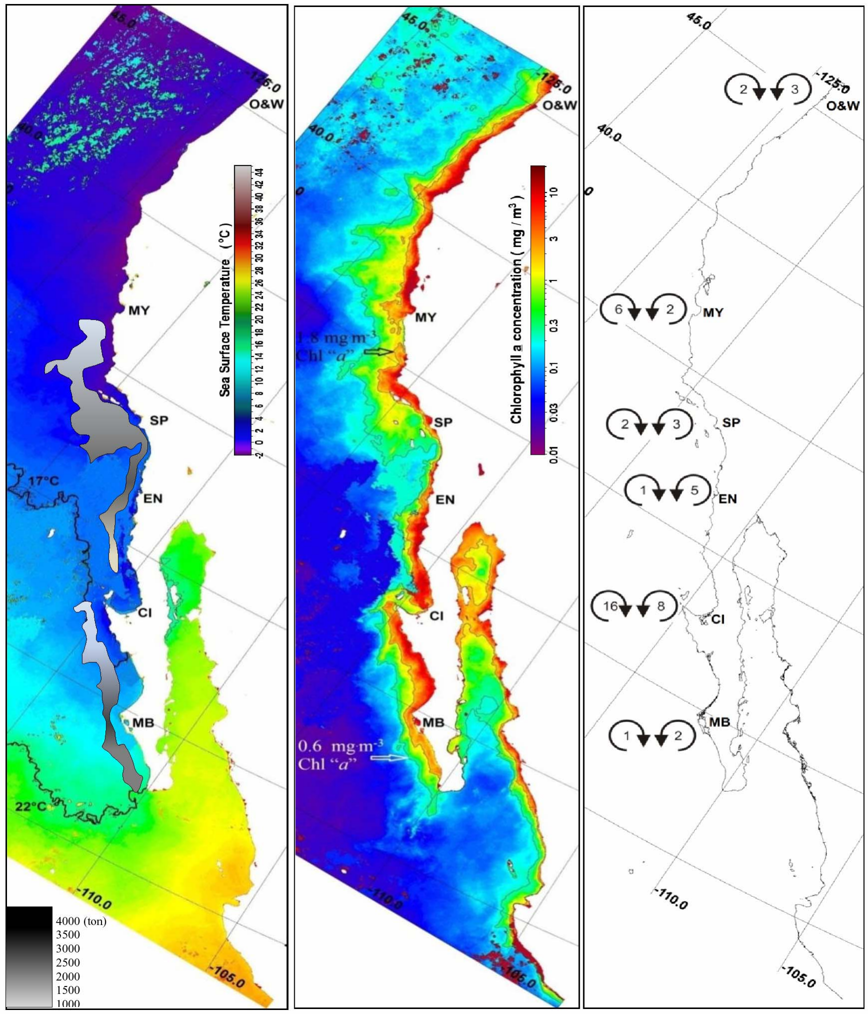


**Figure 6.** Conceptual models of sardine catch distribution for SST and Chl "*a*" (overlaid on winter 2003 images), and mesoscale phenomena for spring. (a) SST seasonal average image overlaid with the stock distribution patterns, and 17°C and 22°C isotherms. (b) Chl "*a*" image with 0.6 and 1.8 mg/m$^3$ isolines. (c) Frequency of mesoscale cyclonic and anticyclonic gyres of each fishing area.

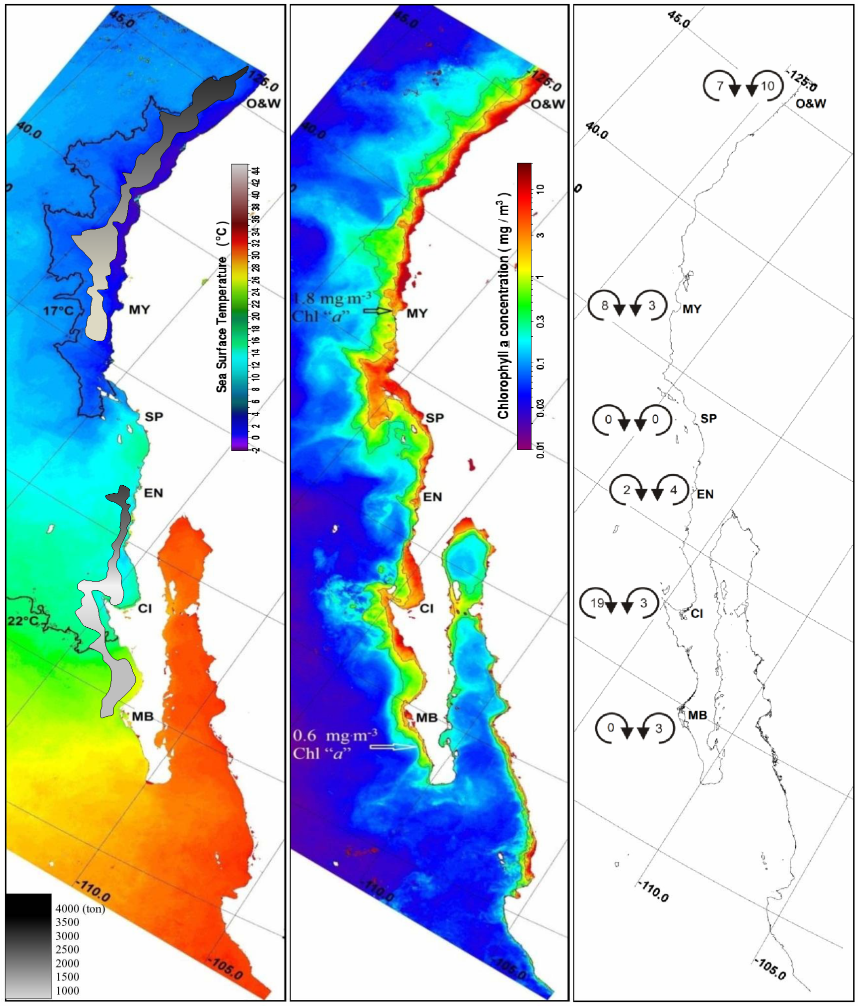


**Figure 7.** Conceptual models of sardine catch distribution for SST and Chl "*a*" (overlaid on winter 2003 images), and mesoscale phenomena for summer. (a) SST seasonal average image overlaid with the stock distribution patterns, and 17°C and 22°C isotherms. (b) Chl "*a*" image with 0.6 and 1.8 mg/m$^3$ isolines. (c) Frequency of mesoscale cyclonic and anticyclonic gyres of each fishing area.

**3.3.3. Summer.** As observed in the conceptual model the two stocks showed a northward displacement from their location in spring (Figure 7a).

The cold stock was observed between O-W and MY but always in areas with SST values below the 17°C isoline. The temperate stock is distributed from EN to MB and mainly in areas with SST between 17°C and 22°C isolines. The higher catches of this season were in O-W (cold stock) and EN (temperate stock).

The catches-Chl "*a*" model showed similar Chl "*a*" values in this season as in spring from SP to O-W but also a decrement from EN to MB (Figure 7b). The maximum catches were obtained again in the range from 0.6 to 1.8 $mg/m^3$. The cold stock maintained in summer its offshore distribution as in spring but the temperate stock presented some movements toward the coast registering also the higher catches offshore between 0.6 to 1.8 $mg/m^3$.

The conceptual model of mesoscale phenomena showed the highest number of cyclonic and anticyclonic gyres of all study present during this season. The catch areas that registered the mayor presence of these phenomena were CI (22), MY (11) and O-W (17) and the minor one was SP (0). The coastal upwellings and filaments maintain their intensity and number as in spring in the northern part of the study area but present a reduction in the southern part.

**3.3.4. Autumn.** According to the catches-SST model both stocks reach the northernmost distribution during this season (Figure 8a). The cold stock is distributed between MY and the northern limit of O-W, and as in the all periods in areas with SST below the 17°C. Most of the temperate stock is found in front of EN in areas with SST between the 17°C and 22°C, but with some presence even to the northern limits of SP, and also in areas with SST values below the 17°C. The higher catches were found to the north of O-W (cold stock) and in EN (temperate stock) with low catches of both stocks in the rest of the areas.

The catches-Chl "*a*" model in this season is similar to the winter between SP and O-W but with a reduction in the concentration to the south of this region and confined to the coast. The higher catches were obtained as in the whole study in the range from 0.6 to 1.8 $mg/m^3$ (Figure 8b).

A drastic reduction of gyres is observed with the conceptual model of mesoscale phenomena in this season being CI the location that registered the mayor number of gyres (9). The coastal upwellings and filaments also reduced their presence and intensity mainly in the southern half of the study area (Figure 8c).

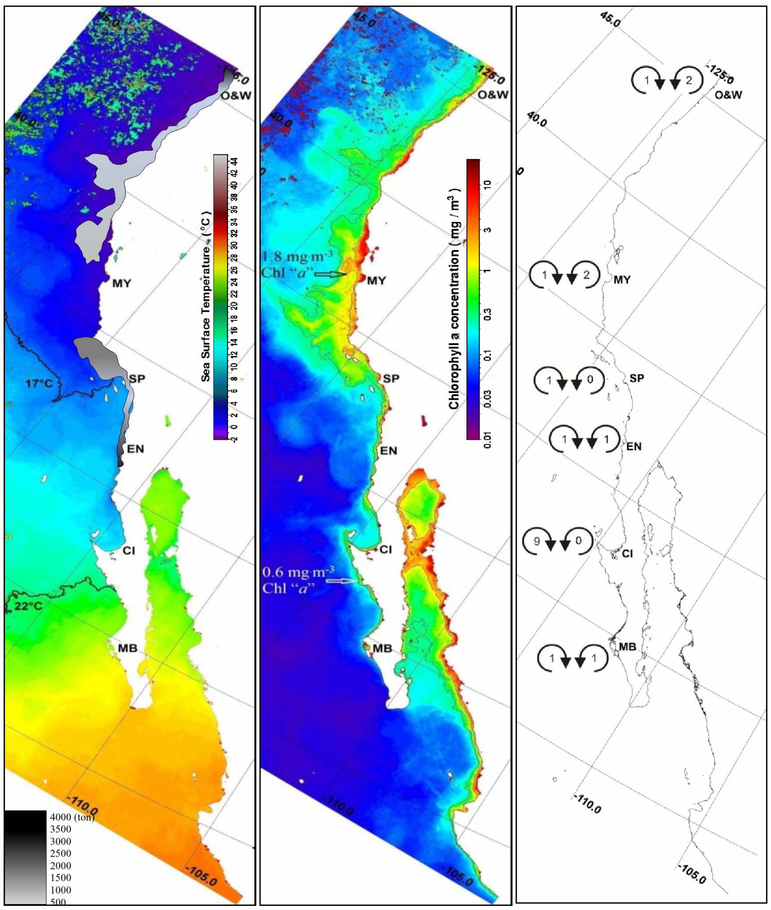


**Figure 8.** Conceptual models of sardine catch distribution for SST and Chl "*a*" (overlaid on winter 2003 images), and mesoscale phenomena for autumn. (a) SST seasonal average image overlaid with the stock distribution patterns, and 17°C and 22°C isotherms. (b) Chl "*a*" image with 0.6 and 1.8 mg/m$^3$ isolines. (c) Frequency of mesoscale cyclonic and anticyclonic gyres of each fishing area.

## 4. Discussion

The results obtained with the application of our space-time distribution models of the Pacific sardine are in accordance with those proposed by Félix-Uraga et al. [20, 21], confirming the existence of 3 stocks adapted to different temperature ranges (cold <17°C, temperate 17°C - 22 °C and warm > 22°C), but being only representative the cold and temperate stocks. In addition to the Félix-Uraga et al. works, we also describe but with better accuracy the location of the stocks in relation to the limits of the temperature ranges and the latitudinal movements of the stocks. Our analysis included as well, an approach of longitudinal movements and a distribution description up to O-W, area not previously described by Félix-Uraga et al. [20, 21], and the limits of Chl "*a*" (0.6 to 1.8 mg/m$^3$) for the both stock distributions. This does not mean that the distribution of this cold stock is limited to the latitude of O-W, but the limitation was the lack of satellite data to analyze the Vancouver fishery.

In relation to the SST variations and catches during the first half of the year, when the cold and temperate stocks are present in their southern distribution, the lowest temperatures coincided with the maximum sardine captures. For the second half of the year, when both stocks moved toward the northernmost part of their distributions, the highest temperatures matches with the catch maxima, coinciding with that described for Félix-Uraga et al. [20, 21]. These authors also defined that the both stock distribution are located in areas with SST range of 17°C-22°C for the temperate stock and lower than 17°C for the cold stock.

Our results in winter suggest that the movement of the two stocks was toward the south which could be related to the intensification of the CC during this season [37]. The distribution of the Chl "*a*" ranges in this season is near to the coast and associated to weak upwellings. In consequence, the higher catches in the fishing areas of MY (cold stock) and MB (temperate stock) were inferred near the coast. The stock distributions are associated to the presence of anticyclonic gyres in MY and cyclonic gyres in MB with less frequency. It is noticeable for the temperate stock zone that while in CI were observed more gyre generation registered scarce catches, but in contrast MB presented lower gyre generation and higher catches, this in spite of the short distance between these locations.

In spring both stocks reach their southernmost distribution, period when the CC reaches their higher intensity and mayor presence towards the south even reaching the PBC [37]. A longitudinal movement of stocks offshore spreading in a mayor area is observed as a consequence of the highest upwelling intensity occurring in this season [37, 52]. The highest catches were observed in EN (cold stock) and MB (tempered stock) associated to cyclonic gyres with a mayor frequency in EN. Furthermore, Ahlstrom [1] and Clark [10, 11] recognize these zones as spawning areas where the larvae have food availability for growth.

The movement to the north of both stocks in summer was evident, period when the CC weakens and the CCC intensifies causing changes in the CCS [14, 37] with the highest frequency of gyres of all seasons. The offshore distribution of both stocks persisted but the highest catches were registered to the north of their distributions (O-W for the cold stock and EN for the temperate one). This situation is due to the persistence of the high upwelling intensity mainly along the coast of USA, and with lesser intensity along the Mexican coast, and the presence of cyclonic gyres with a mayor frequency in O-W. In addition, Emmett et al. [17] and Lluch-Belda et al. [30] considered that the areas occupied by the stocks during summer are used mainly for feeding and sporadic spawning.

In autumn both stocks reach their northernmost distribution when the CCC continues its intensification and the Davidson Current (DC) appears. Some authors suggest that the DC results from the CCC intensification, reaching the surface near the coast and is registered from Pt. Conception to Vancouver [25, 35, 38]. The DC appearance generates a poleward transport of less cold waters to higher latitudes and can contributes that the cold stock be distributed far north reaching the coast of Canada. In other words, we infer that an important part of the cold stock locates beyond the limits of our study area because of the presence of DC in this season, causing a stock displacement to the Vancouver fishing area.

In addition, the weakening of the upwellings during autumn allowed the stocks to move toward the coastal zone. This upwelling decay in the fishing areas has been also observed by Zaytsev et al. [51] and Lynn and Simpson [31] during this season. The tempered stock presented the maximum catches in EN during autumn, in contrast to the cold stock which presented lower catches in all of their distribution area. It is noticeable that in this season was registered the lowest gyres frequency in all fishing areas. In our results we observed a fraction of the temperate stock overpassing its minimum thermal limit of 17°C. In this sense we could assume that this is not part of the temperate stock but a southern fragment of the cold stock as was hypothesized by Emmett et al. [17] and Smith [44].

From the results of this analysis, we infer that sardine stocks are mainly distributed in areas of moderate upwellings throughout the year, and are limited to values between 0.6 to 1.8 $mg/m^3$, which is in agreement with the results obtained by Zwolinski et al. [52] who defined this range as the optimal habitat for this specie.

The productivity changes described with the conceptual models are as a result of the variations of the CCS and the mesoscale physical phenomena [39] consisting of cyclonic and anticyclonic gyres, upwelling and filaments, which are associated to the ocean dynamics of each season [15, 18, 27, 31, 43].

In conclusion, the model allowed us to infer the distribution areas of the Pacific sardine stocks which are linked to the CCS dynamics generating different environmental conditions for each season. Bakun and Broad [3] and Baumgartner and Ferriera-Bartrina [5] consider that areas with high productivity and moderate upwellings determine the distribution and abundance of sardine.

## Acknowledgments

The authors want to thank to Mati Kahru for supplying the complete set of high resolution satellite images. Roberto Félix and Bernardo Shirasago also thank to COFFA and EDI IPN programs for the fellowships. Ricardo Garcia Morales is a recipient of a CONACYT fellowship. Thanks to Bryan Keagle and Ciria Chanel Ceja for editing this manuscript and for their helpful suggestion on the document.

## References

[1] E. H. Ahlstrom, Distribution and abundance of sardine and anchovy larvae in the California current region off California and Baja, California, 1951-64: a summary, U.S. Dept. of the Interior, Fish and Wildlife Service, Washington, D.C., Special Scientific Report: Fisheries No. 534, 1966, 71 pp.

[2] A. Bakun, Patterns in the ocean: ocean processes and marine population dynamics, California Sea Grant/CIBNOR, La Paz, BCS, México, 1996, 323 pp.

[3] A. Bakun, and K. Broad, Environmental “loopholes” and fish population dynamics: comparative pattern recognition with focus on El Niño effects in the Pacific, Fish. Oceanography 12 (2003), 458-473.

[4] H. P. Batchelder, C. A. Edwards and T. M. Powell, Individual-based models of copepod populations in coastal upwelling regions: implications of physiologically and environmentally influenced diel vertical migration on demographic success and nearshore retention, Progress in Oceanography 53 (2002), 307-333.

[5] T. A. Baumgartner and V. Ferriera-Bartrina, Reconstruction of the history of pacific sardine and northern anchovy populations over the past two millennia from sediments of the Santa Barbara Basin, California, CalCOFI Rep. 33 (1992), 24-40.

[6] S. J. Bograd and R. J. Lynn, Long-term variability in the Southern California Current System, Deep-Sea Research II 50 (2003), 2355-2370.

[7] M. E. Carr, Estimation of potential productivity in the Eastern Boundary Currents using remote sensing, Deep-Sea Research II 49 (2001), 59-80.

[8] D. M. Checkley, Jr., R. C. Dotson and D. A. Griffith, Continuous, underway sampling of eggs of Pacific sardine (Sardinops sagax) and northern anchovy (Engraulis mordax) in spring 1996 and 1997 off southern and central California, Deep-Sea Research Part II: Topical Studies in Oceanography 47 (2000), 1139-1155.

[9] F. N. Clark and J. F. Janssen, Movements and abundance of the sardine a measured by tag returns, Calif. Dep. Fish Game Fish Bull. 61 (1945), 7-42.

[10] F. N. Clark, Analysis of populations of the pacific sardine on the basis of vertebral counts, Calif. Dep. Fish Game Fish Bull. 65 (1947), 5-26.

[11] F. N. Clark, Review of the California sardine fishery, Calif. Dep. Fish Game Fish Bull. 38(3) (1952), 367-380.

[12] J. De La Cruz-Agüero and F. J. García-Rodríguez, Morphometric stock structure of the Pacific sardine Sardinops sagax (Jenyns, 1842) off Baja California, Mexico, Morphometrics, Applications in Biology and Paleontology, A. M. Elewa, ed., Springer-Verlag, New York, NY, 2004, pp. 115-124.

[13] E. Di Lorenzo, Seasonal dynamics of the surface circulation in the Southern California Current System, Deep-Sea Research II 50 (2003), 2371-2388.

[14] R. Durazo and T. Baumgartner, Evolution of oceanographic conditions off Baja California: 1997-1999, Progress in Oceanography 54 (2002), 7-31.

[15] R. Durazo, Climate and upper ocean variability off Baja California, Mexico: 1997 2008, Progress in Oceanography 83 (2009), 361-368.

[16] S. Ekman, Zoogeography of the Sea, Sidwick and Jackson Ltd., London, 1953, 417 pp.

[17] R. L. Emmett, R. D. Brodeur, T. D. Miller, S. S. Pool, K. G. Ktutzikowsky, P. J. Bentkey and J. McCrae, Pacific sardine (*Sardinops sagax*) abundance, distribution, and ecological relationships in the Pacific Northwest, CalCOFI Rep. 46 (2005), 122-143.

[18] T. L. Espinosa-Carreon, P. T. Strub, E. Beier, F. Ocampo-Torres and G. Gaxiola-Castro, Seasonal and interannual variability of satellite-derived chlorophyll pigment, surface height, and temperature off Baja California, J. Geophys. Res. 109, C03039, doi:10.1029/2003JC002105, 2004.

[19] P. G. Falkowski and M. J. Oliver, Mix and match: how climate selects phytoplankton, Nat. Rev. Microbiol. 5 (2007), 813-819.

[20] R. Félix-Uraga, V. M. Gómez-Muñoz and W. García-Franco, On the existence of Pacific sardine groups off the west coast of Baja California and Southern California, CalCOFI Rep. 45 (2004), 146-151.

[21] R. Félix-Uraga, V. M. Gómez-Muñoz, C. Quiñonez-Velázquez, F. N. Melo-Barrera, K. T. Hill and W. García-Franco, Pacific sardine (*Sardinops sagax*) stock discrimination off the west coast of Baja California and Southern California using otolith morphometry, CalCOFI Rep. 46 (2005), 113-121.

[22] F. J. Garcia-Rodriguez, S. A. García-Gasca, J. De La Cruz-Agüero, V. M. Cota-Gómez, A study of the population structure of the Pacific sardine *Sardinops sagax* (Jenyns, 1842) in Mexico based on morphometric and genetic analyses, Fisheries Research 107 (2011), 169-176.

[23] G. Gaxiola-Castro, R. Durazo, B. Lavaniegos, M. E. De La Cruz Orozco, E. Millan-Nunez, L. Soto-Mardones and J. Cepeda-Morales, Pelagic ecosystem response to interannual variability off Baja California, Ciencias Marinas 34 (2008), 263-270.

[24] C. Gutiérrez-Flores, Estructura genética poblacional de la sardina del pacífico nororiental *Sardinops sagax caeruleus*, Tesis de Maestría, CICESE, Ensenada, B.C, 2007, 112 pp.

[25] B. Hickey, Coastal oceanography of Western North America from the tip of Baja California to Vancouver Island, A. R. Robinson and K. H. Brink, eds., Coastal Segment, The Sea, Vol. 11, John Wiley & Sons, Inc., New York, 1998, pp. 345-391.

[26] D. Hedgecock, E. S. Hutchinson, G. Li, F. L. Sly and K. Nelson, Genetic and morphometric variation in the Pacific sardine, *Sardinops sagax caerulea*: Comparisons and contrasts with historical data and with variability in the northern anchovy, *Engraulis mordax*, Fishery Bulletin 87(3) (1989), 653-671.

[27] A. Huyer, J. A. Barth, P. M. Kosro, R. K. Shearman and R. L. Smith, Upper-ocean water mass characteristics of the California current, Summer 1993, Deep-Sea Research II 45 (1998), 1411-1442.

[28] D. Kramer and P. E. Smith, Seasonal and geographic characteristics of fishery resources, California current region - VII, Pacific Sardine, Commercial Fisheries Review 33(10) (1971), 7-11.

[29] F. Lecomte, W. S. Grant, J. J. Dodson, R. Rodríguez-Sánchez and B. Bowen, Living with uncertainty: genetic imprints of climate shifts in East Pacific anchovy (*Engraulis mordax*) and sardine (*Sardinops sagax*), Mol. Ecol. 13 (2004), 2169-2182.

[30] D. Lluch-Belda, D. B. Lluch-Cota, S. Hernandez-Vazquez and C. A. Salinas-Zavala, Sardine and anchovy spawning as related to temperature and upwelling in the California Current System, CalCOFI Rep. 32 (1991) 105-111.

[31] R. Lynn and J. Simpson, The California Current system: the seasonal variability of its physical characteristics, J. Geophys. Res. 92(C12) (1987), 12947-12966.

[32] R. Margalef, Life-forms of phytoplankton as survival alternatives in an unstable environment, Ocean. Acta 1 (1978), 493-509.

[33] C. A. Paden, M. R. Abbott and C. D. Winant, Tidal and atmospheric forcing of the upper ocean in the Gulf of California 1. Sea surface temperature variability, J. Geophys. Res. 96(C10) (1991), 18,337-18,359.

[34] W. S. Pegau, E. Boss and A. Martínez, Ocean color observations of eddies during the summer in the Gulf of California, Geophys. Res. Lett. 29(9), 1295, doi: 10.1029/2001GL014076.

[35] A. Pares-Sierra and J. J. O'Brien, The seasonal and interannual variability of the California Current system: a numerical model, J. Geophys. Res. 94 (1989), 3159-3180.

[36] R. H. Parrish, R. Serra and W. S. Grant, The monotypic sardines, *Sardina* and *Sardinops*: Their taxonomy, distribution, stock structure, and zoogeography, Can. J. Fish. Aquat. Sci. 46 (1989), 2019-2036.

[37] P. Perez-Brunius, M. Lopez, A. Pares-Sierra and J. Pineda, Comparison of upwelling indices off Baja California derived from three different wind data sources, CalCOFI 48 (2007), 204-214.

[38] Y. V. Pavlova, Seasonal variations in the California Current, Oceanology 6 (1966), 806-814.

[39] M. H. Pickett and F. B. Schwing, Evaluating upwelling estimates off the west coasts of North and South America, Fish Oceanography 15 (2006), 256-269.

[40] J. L. Reid and R. A. Schwartzlose, Direct measurement of the Davidson current off central California, J. Geophys. Res. 67(6) (1962), 2491-2497.

[41] R. R. Rykaczewski and D. M Checkley, Influence of ocean winds on the pelagic ecosystem in upwelling regions, PNAS 105(6) (2008).

[42] J. J. Simpson and R. J. Lynn, A mesoscale eddy dipole in the offshore California Current, J. Geophys. Res. 95 (1990), 13,009-13,022.

[43] L. Soto-Mardones, A. Pares-Sierra, J. Garcia, R. Durazo and S. Hormazabal, Analysis of the mesoscale structure in the IMECOCAL region (off Baja California) from hydrographic, ADCP and altimetry data, Deep-Sea Res. 51(6-9) (2004), 785-798.

[44] P. A. Smith, A history of proposals for subpopulation structure in the Pacific sardine population off Western North America, CalCOFI Rep., 2005.

[45] P. T. Strub and C. James, Altimeter estimates of anomalous transports into the California Current during 2000-2002, Geophys. Res. Lett. 30(15), 8025, doi: 10.1029/2003GL017513, 2003.

[46] L. D. Talley, Distribution and formation of the North Pacific intermediate water, J. Physical Oceanography 23 (1993), 517-537.

[47] A. M. Vrooman, Serologically differentiated subpopulations of the Pacific sardine, Sardinops caerulea, J. Fish. Res. Board Can. 21 (1964), 691-701.

[48] R. L. Wisner, Evidence of northward movement of stocks of Pacific sardine based on the number of vertebrae, CalCOFI Rep. 8 (1960), 75-82.

[49] R. Wolf and A. E. Daugherty, Age and length composition of the sardine catch off the Pacific Coast of the United States and Mexico in 1961 and 1962, Calif. Fish Game 50 (1964), 241-242.

[50] K. Yoshida and H. L. Mao, A theory of upwelling of large horizontal extent, J. Mar Res. 16 (1957), 40-54.

[51] O. Zaytsev, O. Sanchez-Montante and C. J. Robinson, Características del ambiente hidrofisico de la plataforma continental y zona oceanica adyacente al sistema lagunar Bahia Magdalena-Almejas, R. Funes-Rodriguez, J. Gomez-Gutierrez and R. Palomares-Garcia, eds., Estudios Ecológicos en Bahía Magdalena, CICIMAR-IPN, La Paz, Baja California Sur, Mexico, 2007, pp. 29-43.

[52] J. P. Zwolinski, R. L. Emmett and D. A. Demer, Predicting habitat to optimize sampling of Pacific sardine (Sardinops sagax), ICES J. Marine Science 68 (2011), 867-879.